npg

ORIGINAL ARTICLE

Glucose and oxygen metabolism after penetrating ballistic-like brain injury

Shyam Gajavelli[1], Shimoda Kentaro[1], Julio Diaz[1], Shoji Yokobori[2], Markus Spurlock[1], Daniel Diaz[1], Clayton Jackson[1], Alexandra Wick[1], Weizhao Zhao[1], Lai Y Leung[3], Deborah Shear[3], Frank Tortella[3] and M Ross Bullock[1]

Traumatic brain injury (TBI) is a major cause of death and disability in all age groups. Among TBI, penetrating traumatic brain injuries (PTBI) have the worst prognosis and represent the leading cause of TBI-related morbidity and death. However, there are no specific drugs/interventions due to unclear pathophysiology. To gain insights we looked at cerebral metabolism in a PTBI rat model: penetrating ballistic-like brain injury (PBBI). Early after injury, regional cerebral oxygen tension and consumption significantly decreased in the ipsilateral cortex in the PBBI group compared with the control group. At the same time point, glucose uptake was significantly reduced globally in the PBBI group compared with the control group. Examination of Fluorojade B-stained brain sections at 24 hours after PBBI revealed an incomplete overlap of metabolic impairment and neurodegeneration. As expected, the injury core had the most severe metabolic impairment and highest neurodegeneration. However, in the peri-lesional area, despite similar metabolic impairment, there was lesser neurodegeneration. Given our findings, the data suggest the presence of two distinct zones of primary injury, of which only one recovers. We anticipate the peri-lesional area encompassing the PBBI ischemic penumbra, could be salvaged by acute therapies.

INTRODUCTION

Despite numerous studies on traumatic brain injury (TBI), patient outcomes remain poor. There are approximately 1.5 million patients and 50,000 deaths from TBI every year and many TBI patients survive with disabilities in the United States.[1] Social costs including medical costs and loss of earning capacity are estimated at 48.3 billion dollars a year according to the Centers for Disease Control and Prevention. Penetrating traumatic brain injuries (PTBI) are associated with the worst outcomes and highest death rates of any form of TBI and predominately affect young adults.[2] No therapies, other than surgery, are available for PTBI. There is an urgent need to explore additional treatment options due to epidemic proportions of firearm-related PTBI in modern American society. Florida has had the largest annual firearm-related fatality rate increase in the past decade.[3]

Severity of the primary brain injury determines the prognosis, but its evolution and magnification by secondary damage are also a major influence on outcome. There is now substantial evidence that some secondary brain injury mechanisms such as hypoxia, hypotension, uncontrolled hyperventilation, anemia, and hypoglycemia can be optimally managed in the intensive care unit to influence outcomes. However, there are no definitive drugs/interventions that provide clinical neuroprotection against the progression of primary brain insult, especially for PTBI.[4] Medical and surgical management of PTBI presents a significant challenge to practicing clinicians worldwide.[5] Only recently, aggressive nonspecific management of PTBI with blood products and

hyperosmolar therapy was found to improve survival but with significant disability.[6] As with closed TBI, chemical variations in extracellular glucose, lactate, pyruvate, lactate pyruvate ratio, and brain oxygen tension have been used to guide treatment of PTBI patients.[7–9] In the case of penetrating, firearm-related TBI, the lack of understanding of the underlying pathophysiologic mechanisms hinders the potential effectiveness of these therapeutic interventions, and the development of new neuroprotectants.

Much progress has recently been made with a rat model of PTBI aptly named penetrating ballistic-like brain injury (PBBI). The model captures the rapid temporary brain cavitation caused by a ballistic (bullet or shrapnel) entry into the brain replicating the ensuing secondary pathophysiologic mechanisms that culminate in a permanent cavity with behavioral deficits.[10–14] The PBBI cascade has been summarized temporally into three phases by Williams et al.[12] The first 6 hours after PBBI constitute Phase 1, characterized by rapid elevation in intracranial pressure and reduction in cerebral perfusion pressure. By 5 minutes, hemorrhage, peri-lesional acute transient hypoxia, and cell death from primary injury are evident. Phase 2 spans from 6 to 72 hours and is marked by loss of blood–brain barrier, infiltration of peripheral granulocytes, and a 2.5-fold expansion of the lesion size due to secondary necrosis, apoptosis, and the start of axonal degeneration. Phase 3 occurs from days 3 to 7 and is marked by remote neurodegeneration and scar formation by reactive astrocytes.[12,15]

[1]Department of Neurosurgery, University of Miami, Miller School of Medicine, Miami, Florida, USA; [2]Department of Emergency and Critical Care Medicine, Nippon Medical School, Tokyo, Japan and [3]Brain Trauma Neuroprotection and Neurorestoration, Center for Military Psychiatry and Neuroscience, Walter Reed Army Institute of Research, Silver Spring, Maryland, USA. Correspondence: Professor MR Bullock, Department of Neurosurgery, University of Miami, Miller School of Medicine, Lois Pope LIFE Center, Room 3-20, 1095 NW 14th Terrace, Miami, 33136 FL, USA.
E-mail: RBullock@med.miami.edu

In closed TBI, the cellular changes leading to neurodegeneration have been reviewed previously.[16] Briefly, injury-induced glutamate excitotoxicity results in pollution of mitochondria with calcium, activation of calcium-dependent proteases that initiate cytoskeletal destruction, swelling of mitochondria, release of cytochrome c, dissipation of the mitochondrial membrane potential, mitochondrial dysfunction, increased free radical damage, loss of ATP production, and ionic imbalance culminating in necrosis or apoptosis of neurons. Metabolic responses to TBI have given unexpected insights into how to manage TBI. Global brain metabolism usually decreases after TBI. However, paradoxical increases in glucose metabolism have been detected in some regions of the brain proximal to the impact site.[17] This suggests that hypermetabolic changes might produce more ATP to help the brain restore ionic homeostasis after blunt closed TBI. However, cerebral cellular metabolism after PTBI remains unclear. To assess the metabolic consequences of PTBI, we measured brain oxygen tension, oxygen consumption, and glucose uptake during the acute postinjury phase using the PBBI model. In addition, we investigated the extent to which the observed physiologic and metabolic changes were related to injury-induced neurodegeneration to guide the evaluation of potential of future therapies.

MATERIALS AND METHODS

Surgical Procedures and Penetrating Ballistic-Like Brain Injury

All animal procedures were conducted at the University of Miami, Miller School of Medicine. All procedures were conducted in compliance with guidelines established by the National Institute of Health (NIH) Guide for the Care and Use of Laboratory Animals and were approved by University of Miami's Institutional Animal Care and Use Committee. Adult male Sprague-Dawley rats (250 to 330 g) were used in this study and were maintained on a 12-hour/12-hour light/dark cycle and given food *ad libitum*. Anesthesia was induced with isoflurane (2% to 5%) delivered in a mixture of 70% nitrous oxide and 30% oxygen. Body temperature was maintained at normothermia (37 ± 1°C) throughout all surgical procedures by means of a homeothermic heating system (Harvard Apparatus, South Natick, MA, USA). Food and water were provided *ad libitum* postoperatively.

The sample size calculations, criteria for exclusion/inclusion of injured animals in experiments and randomization of animals into different groups, were performed as described earlier by Williams *et al*.[13] Anesthetized rats were positioned in a stereotaxic device (Kopf, Tujunga, CA, USA) and unilateral PBBI was induced. Briefly, a specially designed stainless steel probe (Popper & Sons Inc., New Hyde Park, NY, USA) with fixed perforations sealed by airtight elastic tubing on one end was mounted to a stereotaxic arm at an angle of 50° from vertical axis and 25° counter-clockwise from anterior-posterior axis. The other end of the probe was connected to a simulated ballistic injury device (Mitre Corp., McLean, VA, USA). The probe was manually inserted through the right frontal cortex of the anesthetized rat via a cranial window (+4.5 mm A-P, +2 mm M-L from bregma) to a distance of 12 mm (from dura). The ballistic component of the injury was induced by a rapid (< 40 ms) water pressure pulse delivered by the injury device, forming an elliptical-shaped balloon calibrated to 10% of the total rat brain volume. After PBBI, the probe was then gently retracted, the cranial opening was sealed with sterile bone wax. Experimental group details are listed in Table 1. The subsequent analyses were performed by staff blinded to the surgery records.

Partial Pressure of Brain Tissue Oxygen Measurement

As described by Murakami *et al*,[18] oxygen probe (Model CC1, 0.5 mm, diameter) and amplifier input of the Licox-MCB device (Integra Lifescience, Plainsboro, NJ, USA) were used for partial pressure of brain tissue oxygen ($PbtO_2$) measurement. The experiment was conducted at optimal fraction of inspired oxygen (FiO_2), i.e., 0.26 to achieve reliable physiologic $PbtO_2$ in anesthetized PBBI rats as close as possible to normal levels.[18] In addition, the femoral artery was cannulated for mean arterial blood pressure measurement using a pressure transducer (#724496, Harvard, Apparatus, Holliston, MA, USA) and for arterial blood gas analysis. Brain temperature was measured using a thermostat probe connected to a dual temperature monitor (model TH-8; Physitemp Instruments, Clifton, NJ, USA). Body

Table 1. Experimental groups, sample size, and figures

#	Measurement	Experimental groups	n/group[a]	Results
1	$PtiO_2$-continous brain O_2 measurement by Licox	Sham	6	Figure 1A
		PBBI	8	Figure 1A
2	Microrespirometry VO_2 measurements	Probe only	10	Figure 1B
		PBBI	10	Figure 1B
3	2-Deoxy glucose (2-DG) mapping of glycolysis	Sham	4	Figure 2
		Probe only	6	Figure 2
		PBBI	8	Figure 2
4	Fluorojade B cell counts	Sham	10	Figure 3
		PBBI	10	Figure 3
5	Hypoperfusion lectin staining	PBBI	3	Figure 4
		Sham	3	Figure 4

Abbreviations: PBBI, penetrating ballistic-like brain injury. [a]Excludes ~ 10% attrition rate for PBBI surgery.

temperature was measured using a rectal probe and the temperature was maintained at 37°C using a heating pad connected to Thermalert (model TH-8; Physitemp Instruments). The animal was positioned in a stereotaxic frame (Kopf) and an incision was made along the mid-line of head. The burr hole for the insertion of $PbtO_2$ and brain temperature probe was drilled at 2.5 mm posterior and 3 mm lateral to the bregma. Each probe was stereotaxically implanted into the right cerebral hemisphere to the depth of 6 mm below the skull surface reaching into the brain region closest to thalamus and entopeduncular nucleus. FiO_2 was measured by a gas analyzer connected to the inspiratory line (AD Instruments, Inc., Colorado Springs, CO, USA). All physiologic signals were digitized and continuously recorded by a PowerLab System (AD Instruments, Inc.).

Microrespirometry

These studies were performed using custom-made 'Cartesian Diver' microrespirometer capable of measuring oxygen consumption (VO_2) from microgram amounts of brain tissue with acceptable accuracy and reproducibility, according to a method published previously.[19] For each animal, five independent data points were measured, three from the ipsilateral injured cortical region and two from the hippocampus, near the lesion and contralateral to the lesion site. The values for the measured VO_2 are reported as μL/h per mg dry weight.

2-Deoxy Glucose Uptake

Two hours after PBBI, a femoral vein was cannulated in the anesthetized rat. Then, immediately before anesthesia was terminated, 50 μCi of [14C] 2-deoxy-D-glucose [14C]DG was administered using a 23-gauge blunt needle *via* the femoral vein over 30 seconds, followed by a 0.2-mL bolus of saline. The anesthesia was then terminated and the animal was allowed to wake up while restrained in a lower body cast to secure the cannulas, as described in Sokoloff *et al*.[20] Blood samples were collected at 20 seconds, 45 seconds, and 85 seconds; and 2 minutes, 3 minutes, 5 minutes, 7 minutes, 12 minutes, 20 minutes, 30 minutes, and 45 minutes after injection to assess serum glucose levels and incorporation of radioactivity. After 45 minutes, the animals were euthanized with 1 mL pentobarbital (60 mg/mL per rat); and the brain was removed as quickly as possible and flash-frozen in isopentane and dry ice. The blood samples were processed and counted with a scintillation counter. The frozen brains were trimmed +2.7 to − 6.3 millimeters embedded in a rat brain matrix, and cut on a dedicated cryostat into 20-μm-thick coronal sections. Three consecutive sections of 300 μm were collected generating a total of 19 series. These serial sections were dried on glass coverslips, glued on poster board, and exposed to [14C]-sensitive PhosphorImaging screens for 36 hours along with [14C] standards of known radioactivity concentration (Amersham Biosciences, Piscataway, NJ, USA). The screens were read and digitized by a PhosphorImaging system (Cyclone Storage Phosphor System; PerkinElmer Life Sciences, Waltham, MA, USA). Individual calibration curves were calculated based on absolute gray levels of the [14C] standards on each film.

Subsequent densitometric measurements were performed by conversion to radioactivity units of nanoCuries per gram (nCi/g). The average metabolic activities in ipsilateral versus contralateral brain were then calculated, using the equations of Sokoloff et al.[20] To generate averaged 2-deoxy glucose (2-DG) distribution maps by using our established image processing procedure,[21] histologic sections were digitized at 8 standardized coronal levels by means of a Xillix CCD-based camera system (with a Nikon macrolens and green filter) interfaced to an MCID image analysis system (Imaging Research, Inc., St Catherines, Ontario, Canada), from which the data were exported to a PC (3 GHz, 4 MB RAM)DEC Alpha workstation for processing.[22]

Fluorojade B Labeling and Unbiased Stereology

Animals were anesthetized, and transcardially perfused, at 24 hours after PBBI. The brains were then isolated and processed for paraffin embedding. Serial coronal brain sections (30 μm thick) were cut through the cerebrum from +4.0 mm to −7.0 mm anterior-posterior to bregma. Serial sections (16 μm thick after shrinkage, 360 μm apart) between bregma levels −4.8 mm and −5.8 mm were stained for Fluorojade B (FJB) (Millipore, Billerica, MA, USA) to identify degenerate neurons.[12] For unbiased stereology, the whole brain and each hemisphere were contoured at ×5 magnification. The physical fractionator method following the workflow on an Axiophot microscope (Carl Zeiss Microlmaging, Inc., Oberkochen, Germany) equipped with StereoInvestigator 7.50.1 software (MicroBrightField, Inc., Williston, VT, USA) was used. A counting grid of 450 μm × 450 μm was placed as to count the number of dead cells estimated using a 60×60-μm counting frame. Then, FJB-positive cells were counted in randomly placed sampling sites with a ×63 objective and multiplied over the entire brain volume between the bregma levels noted above. To enable examination of the relationship between extent of glucose uptake impairment and incidence of neurodegeneration, the data from identical levels were used. To normalize/control for glucose uptake impairment, the numbers of FJB$^+$ cells in a section at a given distance from bregma was divided by the value of glucose uptake for that level.

Lectin Perfusion to Assess Perfusion

Anesthetized rat were transcardially perfused with cold saline, followed by 1% paraformaldehyde followed by DyLight-594-labeled Lycopersicon esculentum lectin (Vector Laboratories, Burlingame, CA, USA). Brains were postfixed in 4% paraformaldehyde and then washed in phosphate-buffered saline (both overnight at 4°C). The brain was sectioned into three blocks. Blocks were incubated (on a rotating shaker at room temperature) in 50%, 80%, and 100% tetrahydrofuran (Sigma, St Louis, MO, USA, 401757) each for 24 hours, and then 100% tetrahydrofuran overnight. The next day, samples were transferred to BABB solution (1:2 ratio of benzyl alcohol, Sigma, 305197; and benzyl benzoate, Sigma, B6630) for

24 hours. After clearing, samples were immediately imaged by LSFM (Ultramicroscope, LaVision BioTec, Bielefeld, Germany). Image analysis and 3D reconstructions were performed using Imaris (Bitplane, Zurich, Switzerland).[23]

Statistical Analysis

All data were expressed as mean ± standard error of the mean. Fluorojade B-positive cell counts and injury volume were analyzed with a one-way analysis of variance (ANOVA), followed by a post hoc Bonferroni's test or test as indicated. Physiologic data and ischemic area were compared using a two-way ANOVA followed by a post hoc Bonferroni's test. Differences were considered as significant at $P < 0.05$. Statistical analysis was performed using GraphPad Prism 5 (GraphPad Software, Inc., La Jolla, CA, USA).

RESULTS

In this study, PBBI induced statistically significant acute transient hypoxia consistent with Murakami et al.[18] (Figure 1A) ($P < 0.05$, $n = 6$ to 8, Multiple t-tests followed by Holm–Sidak method). To examine the consequences of PBBI-induced hypoxia, we used microrespirometry to measure the cerebral rate of oxygen consumption (CMRO$_2$) in cortical tissue cores. In the ipsilateral cerebral cortex between 2.5 and 3.0 hours after PBBI, oxygen consumption was significantly reduced compared with samples from uninjured animals (Figure 1B) ($P < 0.05$, $n = 10$, Mann–Whitney test).

In the brain, oxygen availability influences glucose metabolism, therefore we analyzed global and regional cerebral glucose metabolism. A total of 130 regions of interest from 19 sections, spanning +2.7 mm to −6.3 mm from bregma were examined by ^{14}C autoradiography and rendered as a heat map (see Materials and methods). Color-coded maps of local cerebral metabolic rate of glucose (LCMR$_{glu}$) perfectly overlapped with the histologic descriptions of the PBBI (Figure 2A).[13] The mean glucose utilization over the entire brain (sum of all 19 sections) for the sham, probe (no inflation), and PBBI treatment groups was 3,075.95, 3,098.73, and 1,784.29 μmol/100 g per minute, respectively. Total cerebral glucose uptake was significantly reduced by the injury (PBBI) compared with sham groups ($P < 0.05$) (F = 19.33) and probe-only groups (no-inflation control). Additionally, there was no statistically significant difference between sham groups and probe-only groups ($n = 4$ to 5/group, one-way ANOVA followed by Bartlett's test) (Figure 2B). The core of the injury could be clearly visualized as an oval cavity with the lowest 2-DG
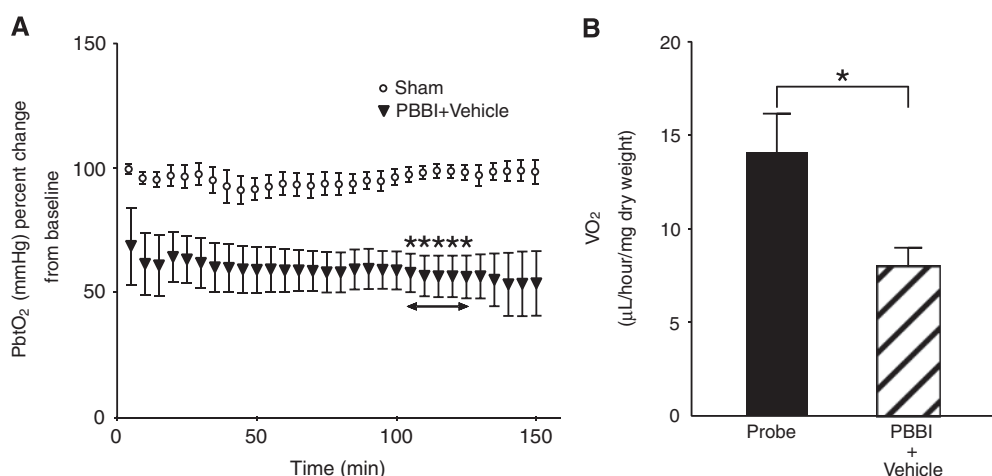

Figure 1. Cerebral oxygen metabolism after penetrating ballistic-like brain injury (PBBI). (**A**) Time course of brain hypoxia. There were significant differences in partial pressure of brain tissue oxygen (PbtO$_2$) percent from baseline between sham and PBBI groups from 105 to 125 minutes after injury (asterisk, $P < 0.05$). (**B**) Brain tissue oxygen consumption in ipsilateral cortex. There was a significant difference in VO$_2$ between probe and PBBI groups 2.5 hours after injury ($P < 0.05$).
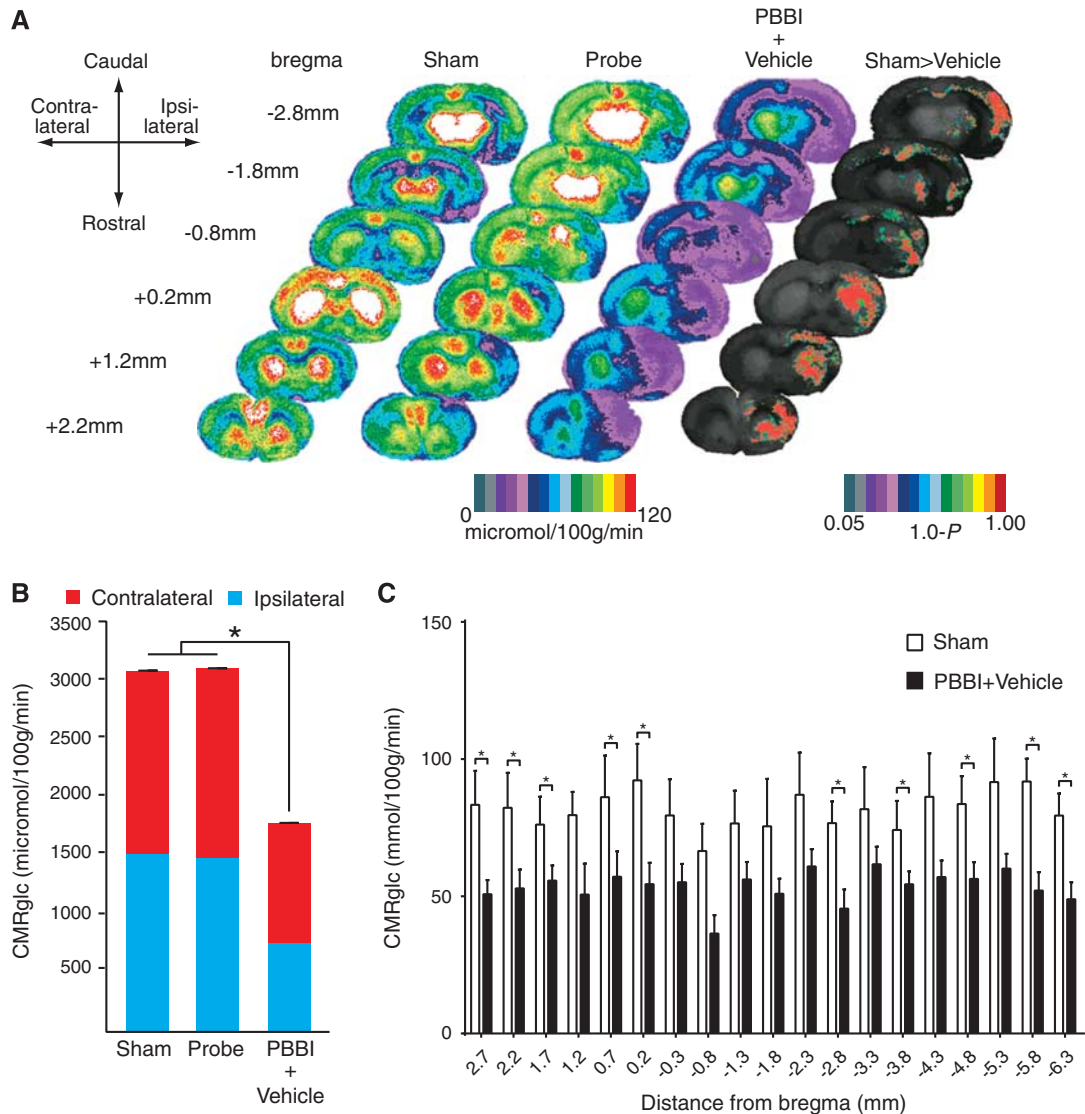
Figure 2. Local cerebral glucose metabolism after penetrating ballistic-like brain injury (PBBI). (**A**) Color-coded maps of average local cerebral metabolic rate for glucose (LCMR$_{glc}$) at 2.5 hours after injury. Each coronal section is a representation of multiple animals within a group: Sham $n = 4$, Probe $n = 5$, PBBI $n = 10$. Atlas levels are given on the left column and represent the longitudinal distance between each section and the bregma in millimeters. Positive and negative values indicate distances in the anterior and posterior directions, respectively. Compared with controls (columns 1 and 2) in PBBI (column 3), LCMR$_{glc}$ decreased radially from injury core into perilesional areas and globally across the entire brain. In control (Probe only group), hypoglycolysis was limited to anterior half corresponding to the entrance route of the probe. P-maps of average local cerebral glucose utilization were produced by comparing the values of pixels corresponding to the same anatomic position across groups. The color-coded pixels shown here are those found to be significantly different ($P < 0.05$) in a pairwise comparison between two groups (Sham versus PBBI). Greater-than symbols ($>$) indicate the directionality of the results. The P was subtracted from 1.0 so that the highest value on the scale represents $P = 0$, and the lowest $P \geqslant 0.05$. (**B**) Comparison of glucose utilization in whole brain between Sham and PBBI groups. There was a significant decrease in LCMR$_{glc}$ of whole brain between Sham and PBBI groups ($P < 0.05$, $n = 4$ to 5/group, ordinary one-way ANOVA). Greater impairment of glucose uptake was observed in the ipsilateral than the contralateral hemisphere. (**C**) Comparison of glucose uptake across rostrocaudal axis. There were significant decreases in LCMRglc between sham and PBBI groups in brain sections at 2.7 , 2.2, 1.7 , 0.7, 0.2, -2.8, -3.8, -4.8, -5.8, and -6.3 mm from bregma in the ipsilateral hemisphere ($P < 0.05$, $n = 4$ to 5/group, Multiple *t*-tests followed by Holm–Sidak method). *P < 0.05 t-test followed by Holm Sidak.

values (PBBI versus Sham groups; Figure 2A). After insertion of the probe alone (with no balloon inflation) reductions in 2-DG uptake were limited to anterior brain regions, corresponding to the entrance route of the probe (Probe-only group; Figure 2A). Although the injury was unilateral, it resulted in bilateral hypoglycolysis: Sham Ipsi versus PBBI Ipsi (with mean difference of 39.92), and Sham Ipsi versus PBBI Contra (with mean difference of 26.75), Sham Contra versus PBBI Contra (with mean difference of 28.06). Interestingly, a trend for hypoglycolysis was also limited

to the anterior and posterior length of the injury tract (Figure 2C). Multiple *t*-tests were used to compare the 2-DG uptake in sections between groups. Glucose metabolism after PBBI was reduced bilaterally in a number of brain regions including the cingulate cortex, frontal cortex, parietal cortex, ventrolateral orbital cortex, nucleus accumbens, caudate putamen, dorsal agranular insular cortex, intermediate and lateral septal nuclei, limb cortical areas, globus pallidus, posterior agranular cingular cortex, retrosplenial cortex, hippocampus, striatum, occipital cortex, temporal cortex,

central gray, and dentate gyrus. The levels of glucose in peripheral circulation were unaltered between groups (data not shown).

Neurodegenerative cell counts 24 hours after PBBI were compared between PBBI rats and uninjured rats. Increased evidence of neurodegeneration was detected in the injury core and in the peri-lesional zone of the injured hemisphere (Figure 3A). Verification of neurodegeneration by Fluorojade staining is shown in Figure 3B. In the ipsilateral hemisphere, the number of FJB+ cells was significantly greater than that in the contralateral hemisphere ($P = 0.0152$, $n = 6$, Mann–Whitney test GraphPad Prism 6.0, GraphPad Software, Inc., La Jolla, CA, USA, Figure 3D). To assess status of microvasculature after PBBI, we combined fluorescent lectin perfusion with light sheet microscopy. A composite image of the each hemisphere shows the extent of lectin labeling (hence perfusion) (Figures 4A and 4B). Compared with the contralateral side, hypoperfusion was evident on the ipsilateral hemisphere (values for lectin labeling volume $6.4E10\,\mu m^3$ versus $4.6E10\,\mu m^3$, respectively (Figure 4A). Surface reconstruction using Imaris software clearly shows the absence of perfusion of a major blood vessels ipsilateral to the injury in contrast to the contralateral side (Figure 4A). This region of hypoperfusion also shows least uptake of 2-DG and corresponds to the center of the injury tract. This is rostro-caudally flanked by regions with higher 2-DG uptake

(Figure 4C). The cortical neurodegeneration (FJB staining) data across five evenly spaced brain sections spanning (−0.3 mm to − 4.3 mm from bregma, $n = 6$/group) were compared with the 2-DG uptake data to explore the possible existence of a penumbra (Figure 4D). The 2-DG uptake was least in the cortex at − 0.8 mm and − 2.8 mm from bregma (Figure 4C). In contrast, the FJB+cell counts peaked at − 0.3 mm but decreased exponentially caudally at − 4.3 mm from bregma. The FJB/LCMR$_{glc}$ ratio across the sections revealed the numbers of FJB+ cells at the injury core decreased from 100% at − 0.3 mm to 8% at − 4.3 mm from bregma. In the brain sections (−0.3 mm to − 1.3 mm) recovery may be hampered due to severe ischemia as evidenced by lack of a capillary network (Figures 4A and 4B) < 31% of maximal LCMR$_{glc}$ thus constitute the irrecoverable injury core (** in Figure 4C). While in the flanking regions (−2.3 mm to − 4.3 mm from bregma) there is robust recovery from ischemia as evidence by lower FJB counts (Figure 4D). Taken together, this region could constitute the penumbra (* in Figure 4C).

DISCUSSION

The passage of a high velocity projectile (e.g., bullet or shrapnel) through the brain produces intense local shearing forces,
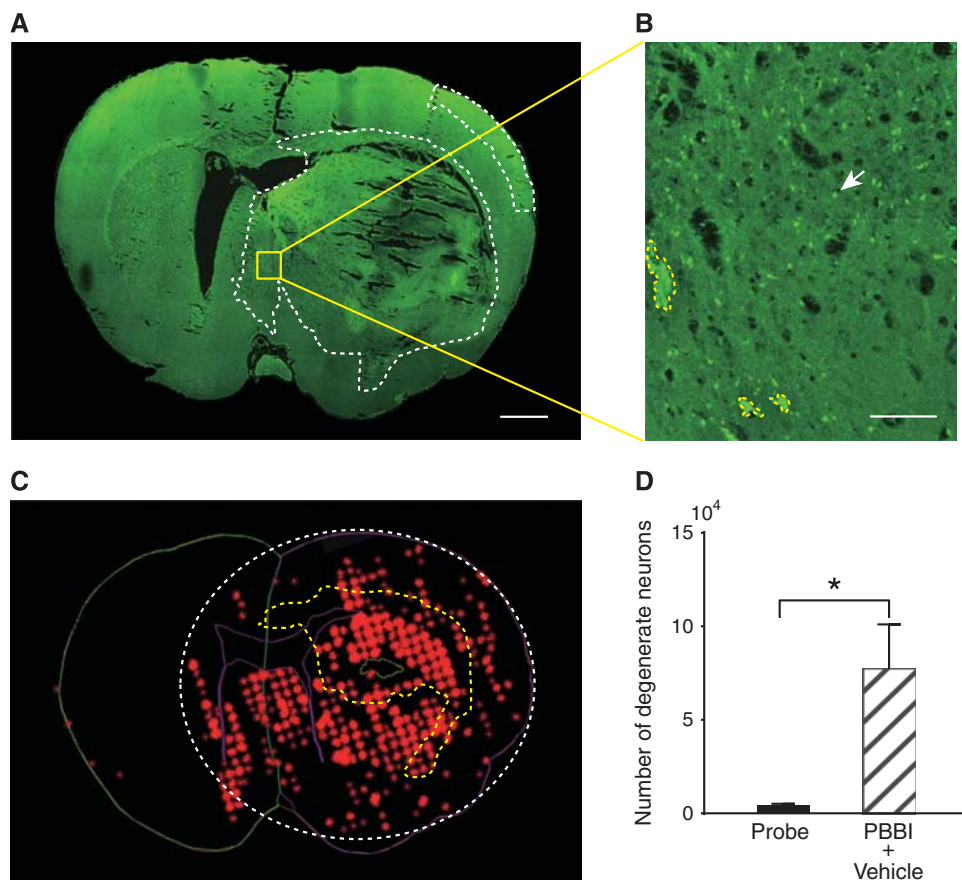

Figure 3. Neurodegeneration after penetrating ballistic-like brain injury (PBBI). (**A**) A confocal image of a Fluorojade B (FJB)-stained coronal section at 0.8 mm distance from bregma shows regions with FJB+ cells (circumscribed by white-dotted line). Greater neurodegeneration was observed in the injury core and peri-injury zone in the ipsilateral than those in the contralateral cerebral cortex. (**B**) A higher magnification of the region outlined in (**A**) shows representative FJB+ cell (white arrow) and blood clot (circumscribed by yellow-dotted line). (**C**) The image represents various contours used for unbiased stereological quantification of FJB+ cells. The contralateral hemisphere is outlined in green. The ipsilateral hemisphere and lateral ventricles are outlined in purple. Red asterisks are used to mark individual FJB+ cells that appear as clusters. Intracranial hemorrhage is circumscribed by a yellow-dotted line. White-dotted line circumscribes the area containing FJB+ cells. Bar = 1 mm (**A**), 100 μm (**B**). (**D**) Quantification of neurodegeneration after PBBI. There was a significant difference in the number of FJB+ cells between probe and PBBI groups in the ipsilateral hemisphere ($P < 0.05$, $n = 6$/group, Mann–Whitney test). *$P < 0.05$, Mann-Whitney.
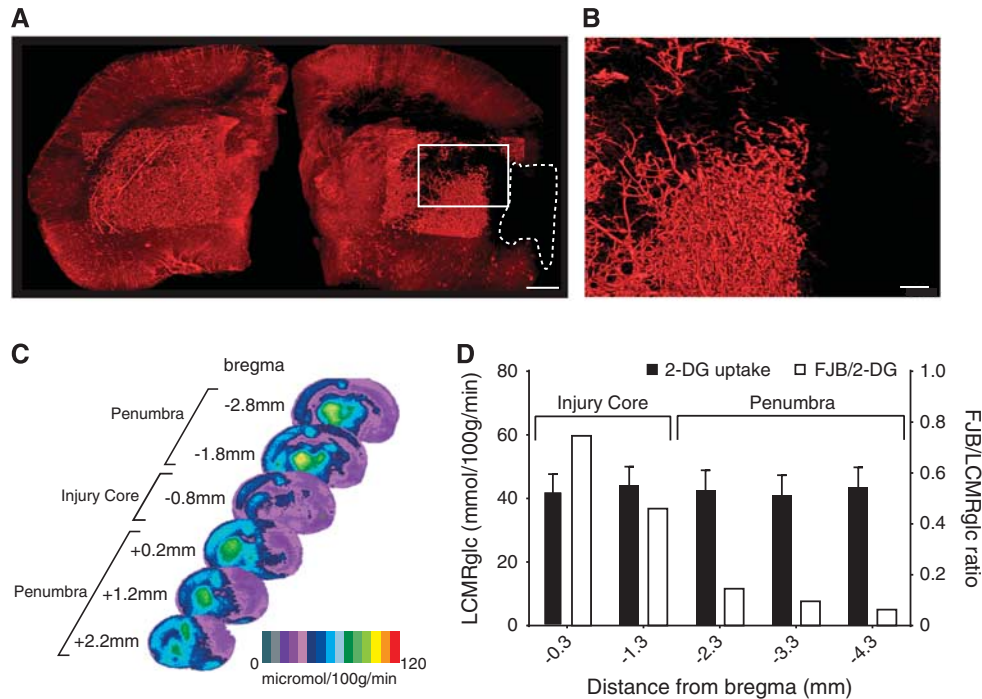
Figure 4. (**A**) A composite light sheet microscopy image shows ipsi and contralateral hemispheres 0.5-mm-thick section between −0.9 mm and −1.4 mm from bregma of penetrating ballistic-like brain injury (PBBI) brain (at 2.5 hours) perfused with fluorescent tomato-lectin at 0.8 mm distance from bregma. Region with injury induced hypoperfusion is circumscribed by white-dashed line. Surface reconstruction renders the labeled vasculature in 3D. (**B**) A higher magnification of the region outlined in (**A**) shows a progressive decrease in vascular labeling. (**C**) Hypoperfused region overlaps with the 2-deoxy glucose (2-DG) uptake impairment heat map. The injury core (**) and in regions rostral (*) and caudal (*) are equally impaired. (**D**) The incidence of neurodegeneration was proportional to 2-DG uptake impairment at the injury core but not in regions caudal to the injury core. Fluorojade B (FJB)/$LCMR_{glc}$ ratio decreased from injury core toward more caudal regions, decreasing maximally at −2.3 mm from bregma and plateaued (penumbra). $LCMR_{glc}$, local cerebral metabolic rate of glucose.

especially adjacent to the compression/cavitation zone and which progress along the entire course of the injury tract. When the projectile is of a sufficient mass and velocity, the entire brain is affected, and death is usually rapid, as seen in high velocity rifle wounds. However, when the mass of the projectile or its velocity is low enough to restrict the compression/cavitation damage zone to a smaller tissue zone in the brain, as seen in handgun victims and those injured through shrapnel, etc., the PBBI rat model depicts the neuropathologic consequences of these survivable PTBI injuries in humans, with a high degree of accuracy.[13]

The delayed nature of cell death, over weeks or months in humans, and over days in rats, is well known.[24,25] However, no therapies have been shown to influence this process. As part of a Department of Defense-funded effort to gain insights into mechanisms underlying PTBI, we have determined the oxygen tension ($PbtO_2$), oxygen consumption ($CMRO_2$), glucose uptake (2-DG method), and their relationship to regional cell death in the PBBI rat model.

Hypoxia is also associated with deficits in $CMRO_2$ both in TBI patients and in experimental TBI. The results of the current study provide the first demonstration of acute impaired $CMRO_2$ in the PBBI model (Figure 1). This apparent hypoxia occurs in limited range of FiO_2 (0.26 to 0.30). This range was used as it facilitated maintenance of clinically relevant pH and pCO_2.[18] Partial pressure of brain tissue oxygen assessment in PBBI animals under normoxia, and hyperoxia with acceptable pH and pCO_2 would provide clinically relevant insights into the nature of observed acute hypoxia. The microrespirometry assay is performed in the presence of oxygen and glucose, hence lower $CMRO_2$ after PBBI suggests 'mitochondrial dysfunction' similar to that seen in PTBI patients.[19,26] Acute hypoxia and lowered $CMRO_2$ after PBBI are

consistent with PTBI patient data and previous work in PBBI.[7,9,18] However, there is no precedent to targeting $CMRO_2$ after PTBI to improve outcomes On the basis of the PBBI literature and findings in this study, it can be expected that PTBI-induced mitochondrial dysfunction may limit benefits from manipulation of $CMRO_2$. Yao *et al*[27] compared tissue viability after PBBI and middle cerebral artery occlusion using TTC (2,3,5-triphenyltetrazolium chloride) staining and found that, unlike middle cerebral artery occlusion, TTC staining after PBBI was preserved at 24 hours after injury.[27] The TTC staining is a measure of mitochondrial oxidative phosphorylation complex I activity and the absence of staining reflects tissue ischemia.[28] Therefore, PBBI appears to induce a metabolic defect that is between the oxidative phosphorylation complex I (based on intact TTC) and complex IV (based on reduced $CMRO_2$). The persistence of oxidative phosphorylation complex I activity in the absence of oxygen consumption may increase production of reactive oxygen species contributing to PBBI-induced neurodegeneration. In contrast to stroke and closed TBI where there was an initial increase followed by a decrease in $CMRO_2$, in PBBI there is only a decrease. On the basis of these data, it may be speculated that damage to the mitochondria in the PBBI compression/cavitation zone triggers the mechanical release of well-characterized factors such as cytochrome c, or novel factors such as inflammasomes that increase apoptosis and necrosis in the neighboring tissues and spreading mitochondrial dysfunction to areas beyond the primary injury.[29,30]

Importantly, astrocyte-mediated transcellular mitophagy has recently been implicated as a mechanism that helps maintain neuronal metabolism.[31] However, the degree to which increased intracranial pressure and reactive gliosis may impair intra/transcellular mitophagy after PBBI is not yet known. Before

manipulating oxygen levels, targeted mitochondrial stability/biogenesis may be necessary. Preclinical work has shown that mitochondrial uncoupling after injury may be beneficial by reducing reactive oxygen species production, albeit the downside of such intervention (i.e., hyperthermia) needs to be mitigated.[32] Alternatively, increased clearance of dysfunctional mitochondria by transcellular mitophagy may serve as a better antioxidant than any extraneous agents with antioxidant activity. Given our findings, there is no evidence to suggest that manipulation of brain oxygen tension alone can improve PTBI outcomes.

In the current study, significant decreases in glucose uptake were detected both globally and in a region-specific manner after PBBI in rats. To our knowledge, these findings are the first reports to show a profound global decrease in glucose uptake after PBBI. Previous studies using brain injury models reported an acute period of increase glucose metabolism on the order of minutes.[33] In our study, the metabolic measurements were made hours after the insult. Therefore, the period of hyperglycolysis might have been missed hence cannot be ruled out. Another caveat that needs consideration is that compared with TBI, PBBI injury may have relatively greater compromise of blood–brain barrier. In TBI patients and the fluid percussion injury model of closed head injury, less severe regional decreases in cerebral metabolic rate of glucose were seen using ^{13}C nuclear magnetic resonance spectroscopy and ^{18}F-fluorodeoxyglucose positron emission tomography, and using the 2-DG method, in animal models, such as fluid percussion injury. Similarly, in a stroke model (reversible middle cerebral artery occlusion) glucose utilization is decreased regionally, and a core lesion of depressed 2-DG uptake is surrounded by a zone of increased 2-DG uptake. In contrast, in this study at the time pointed tested we could not observe any regions of hyperglycolysis, after PBBI.

Under normal physiologic conditions oxygen helps degrade hypoxia inducible factor 1α while hypoxia stabilizes it. Hypoxia inducible factor 1α associates with a basic helix–loop–helix transcription factor to upregulate genes encoding enzymes involved in cellular metabolism, including the glycolytic enzymes.[34] Despite acute hypoxia, the hypoxia inducible factor 1α protein is not detectable ipsilateral to the injury after PBBI (unpublished data and Cartagena et al[35]). The absence of hyperglycolysis in PBBI is consistent with lack of hypoxia inducible factor 1α. Thus, the use of glucose or lactate to supplement metabolism may rescue the 'PBBI penumbra' tissue surrounding the injury core.[8] Global reduction of glucose utilization could be due to the much larger lesion volume in PBBI than that in closed TBI, fluid percussion injury, and stroke models in the rat.

The reasons for decreased glucose uptake after PBBI could be similar to those seen in TBI such as poor perfusion, glucose transport across the blood–brain barrier, diminished hexokinase activity, and severe loss of cerebral perfusion pressure after PBBI.[15] To test whether poor perfusion underlies the phenomenon, we assessed the density of the microvasculature using a tomato-lectin over multiple time points. We found significant progressive decrease in vascular labeling compared with controls up to a week after PBBI (Figure 4A). Taken together, significant global hypoglycolysis and persistent loss of the capillary network, as seen in this study, are consistent with a permanent ischemia-like state, as seen after vessel occlusion, in stroke. One limitation of extending these findings to PTBI is that the PBBI mathematical models the intracranial cerebral temporary cavitation, tissue tearing and shearing accurately capturing the secondary events. However, the model does not model the rapid entry of projectile and associated metabolic consequences. The injury is proportional to the balloon expansion and consequent secondary mechanisms.[10–13,15,27,36]

Experimental studies using stroke models to document the ischemic flow thresholds of brain tissue have showed the existence of two critical levels of decreased perfusion: first, a level representing the flow threshold for reversible functional failure (functional threshold); second, a lower threshold below which irreversible membrane failure and morphologic damage occur.[22] In PBBI, demonstrating the presence of an ischemic penumbra region, and its severity, could help improve outcomes. For example, reduced glycolysis may suggest that lactate or ketone administration may be beneficial.[17] For this reason, we assessed the relationship between depression of 2-DG uptake and extent of cortical neurodegeneration at multiple bregma levels. Neurodegeneration as assessed using FJB has been found to peak from 24 to 72 hours after PBBI. This result is similar to previous report and indicates that neuronal cell death occurs primarily ipsilateral after PBBI.[12] Due to technical limitations, 2-DG uptake and labeling for neurodegeneration (FJB) were performed in separate groups of animals. However, anatomically homologous sections from bregma were matched using hematoxylin and eosin stained sections. The hypoperfusion, hypoxia, decreased glucose uptake, acute impaired cerebral oxygen consumption (2.5 hours after injury) culminate to produce neurodegeneration at the PBBI injury core (at 24 hours after injury). Despite the aforementioned pathophysiologic contributors, rostrocaudally from the injury epicenter there is lower neurodegeneration suggesting similarities to stroke penumbra (Figure 4D), where studies in ischemic stroke models suggest that such a region is characterized by low perfusion, electrical silence, and damaged but viable neurons that can be putatively rescued by early thrombolytic therapy.[37,38] Consistent with our PBBI $CMRO_2$ and $LCMR_{glc}$ results, a positron emission tomography study of closed TBI patients has shown a decrease in CBF, oxygen extraction fraction, $CMRO_2$, and $LCMR_{glc}$, with anaerobic metabolism in the hypodense gray matter at the pericontusional area.[39]

To better guide future therapeutic strategies for PTBI, we have focused on elucidating the pathophysiology. Our data show significant reductions in glucose utilization in the whole brain hemisphere occurring concomitantly with significant decreases of cerebral oxygen consumption and consequent neurodegeneration localized to the 'core lesion' (albeit using different animals). The metabolic impairments appear to be tied to impaired perfusion and spontaneous recovery from the early PBBI metabolic impairments is apparent at 24 to 72 hours after injury. Brain regions that show evidence of injury-induced mitochondrial dysfunction transition into neurodegeneration, whereas regions absent of mitochondrial impairment remain free of neurodegeneration. These data suggest that, unlike in closed TBI, use of normobaric hyperoxia or hyperbaric oxygen as a clinical intervention may produce mixed results in PTBI. However, as reported earlier for both PBBI and acute subdural hematoma, hypothermia may provide to be a better option.[16,40] Gradual metabolic restoration via slow rewarming giving injured tissue time to carry out repairs (such as mitochondrial biogenesis) and reverse metabolic derangements is theoretically attractive extrapolation of our data.

DISCLOSURE/CONFLICT OF INTEREST

ACKNOWLEDGMENTS

REFERENCES

1 Coronado VG1, Xu L, Basavaraju SV, McGuire LC, Wald MM, Faul MD et al. Centers for Disease Control and Prevention (CDC). Surveillance for traumatic brain injury-related deaths--United States, 1997-2007. *MMWR Surveill Summ* 2011; **60**: 1–32.

2 Cavaliere R, Cavenago L, Siccardi D, Viale GL. Gunshot wounds of the brain in civilians. *Acta Neurochir (Wien)* 1988; **94**: 133–136.

3 Kalesan B, French C, Fagan JA, Fowler DL, Galea S. Firearm-related hospitalizations and in-hospital mortality in the United States, 2000-2010. *Am J Epidemiol* 2014; **179**: 303–312.

4 Fu ES, Tummala RP. Neuroprotection in brain and spinal cord trauma. *Curr Opin Anaesthesiol* 2005; **18**: 181–187.

5 Kazim SF, Shamim MS, Tahir MZ, Enam SA, Waheed S. Management of penetrating brain injury. *J Emerg Trauma Shock* 2011; **4**: 395–402.

6 Joseph B, Aziz H, Pandit V, Kulvatunyou N, O'Keeffe T, Wynne J et al. Improving survival rates after civilian gunshot wounds to the brain. *J Am Coll Surg* 2014; **218**: 58–65.

7 De Fazio M, Rammo R, O'Phelan K, Bullock MR. Alterations in cerebral oxidative metabolism following traumatic brain injury. *Neurocrit Care* 2011; **14**: 91–96.

8 Glenn TC, Kelly DF, Boscardin WJ, McArthur DL, Vespa P, Oertel M et al. Energy dysfunction as a predictor of outcome after moderate or severe head injury: indices of oxygen, glucose, and lactate metabolism. *J Cereb Blood Flow Metab* 2003; **23**: 1239–1250.

9 Henry B, Emilie C, Bertrand P, Erwan D. Cerebral microdialysis and PtiO2 to decide unilateral decompressive craniectomy after brain gunshot. *J Emerg Trauma Shock* 2012; **5**: 103–105.

10 Williams AJ, Wei HH, Dave JR, Tortella FC. Acute and delayed neuroinflammatory response following experimental penetrating ballistic brain injury in the rat. *J Neuroinflammation* 2007; **4**: 17.

11 Williams AJ, Ling GS, Tortella FC. Severity level and injury track determine outcome following a penetrating ballistic-like brain injury in the rat. *Neurosci Lett* 2006; **408**: 183–188.

12 Williams AJ, Hartings JA, Lu XC, Rolli ML, Tortella FC. Penetrating ballistic-like brain injury in the rat: differential time courses of hemorrhage, cell death, inflammation, and remote degeneration. *J Neurotrauma* 2006; **23**: 1828–1846.

13 Williams AJ, Hartings JA, Lu XC, Rolli ML, Dave JR, Tortella FC. Characterization of a new rat model of penetrating ballistic brain injury. *J Neurotrauma* 2005; **22**: 313–331.

14 Shear DA, Lu XC, Bombard MC, Pedersen R, Chen Z, Davis A et al. Longitudinal characterization of motor and cognitive deficits in a model of penetrating ballistic-like brain injury. *J Neurotrauma* 2010; **27**: 1911–1923.

15 Wei G, Lu XC, Yang X, Tortella FC. Intracranial pressure following penetrating ballistic-like brain injury in rats. *J Neurotrauma* 2010; **27**: 1635–1641.

16 Yokobori S, Gajavelli S, Mondello S, Mo-Seaney J, Bramlett HM, Dietrich WD et al. Neuroprotective effect of preoperatively induced mild hypothermia as determined by biomarkers and histopathological estimation in a rat subdural hematoma decompression model. *J Neurosurg* 2013; **118**: 370–380.

17 Prins M, Greco T, Alexander D, Giza CC. The pathophysiology of traumatic brain injury at a glance. *Dis Model Mech* 2013; **6**: 1307–1315.

18 Murakami Y, Wei G, Yang X, Lu XC, Leung LY, Shear DA et al. Brain oxygen tension monitoring following penetrating ballistic-like brain injury in rats. *J Neurosci Methods* 2012; **203**: 115–121.

19 Levasseur JE, Alessandri B, Reinert M, Bullock R, Kontos HA. Fluid percussion injury transiently increases then decreases brain oxygen consumption in the rat. *J Neurotrauma* 2000; **17**: 101–112.

20 Sokoloff L, Reivich M, Kennedy C, Des Rosiers MH, Patlak CS, Pettigrew KD et al. The [14C]deoxyglucose method for the measurement of local cerebral glucose utilization: theory, procedure, and normal values in the conscious and anesthetized albino rat. *J Neurochem* 1977; **28**: 897–916.

21 Zhao W, Ginsberg MD, Smith DW. Three-dimensional quantitative autoradiography by disparity analysis: theory and application to image averaging of local cerebral glucose utilization. *J Cereb Blood Flow Metab* 1995; **15**: 552–565.

22 Back T, Zhao W, Ginsberg MD. Three-dimensional image analysis of brain glucose metabolism-blood flow uncoupling and its electrophysiological correlates in the acute ischemic penumbra following middle cerebral artery occlusion. *J Cereb Blood Flow Metab* 1995; **15**: 566–577.

23 Jahrling N, Becker K, Dodt HU. 3D-reconstruction of blood vessels by ultramicroscopy. *Organogenesis* 2009; **5**: 227–230.

24 Maxwell WL, MacKinnon MA, Stewart JE, Graham DI. Stereology of cerebral cortex after traumatic brain injury matched to the Glasgow outcome score. *Brain* 2010; **133**: 139–160.

25 Bramlett HM, Dietrich WD. Quantitative structural changes in white and gray matter 1 year following traumatic brain injury in rats. *Acta Neuropathol* 2002; **103**: 607–614.

26 Verweij BH, Muizelaar JP, Vinas FC, Peterson PL, Xiong Y, Lee CP. Impaired cerebral mitochondrial function after traumatic brain injury in humans. *J Neurosurg* 2000; **93**: 815–820.

27 Yao C, Williams AJ, Ottens AK, Lu XC, Liu MC, Hayes RL et al. P43/pro-EMAPII: a potential biomarker for discriminating traumatic versus ischemic brain injury. *J Neurotrauma* 2009; **26**: 1295–1305.

28 Tsukada H, Ohba H, Nishiyama S, Kanazawa M, Kakiuchi T, Harada N. PET imaging of ischemia-induced impairment of mitochondrial complex I function in monkey brain. *J Cereb Blood Flow Metab* 2014; **34**: 708–714.

29 Sullivan PG, Keller JN, Bussen WL, Scheff SW. Cytochrome c release and caspase activation after traumatic brain injury. *Brain Res* 2002; **949**: 88–96.

30 de Rivero Vaccari JP, Dietrich WD, Keane RW. Activation and regulation of cellular inflammasomes: gaps in our knowledge for central nervous system injury. *J Cereb Blood Flow Metab* 2014; **34**: 369–375.

31 Davis CH, Kim KY, Bushong EA, Mills EA, Boassa D, Shih T et al. Transcellular degradation of axonal mitochondria. *Proc Natl Acad Sci USA* 2014; **111**: 9633–9638.

32 Pandya JD, Pauly JR, Sullivan PG. The optimal dosage and window of opportunity to maintain mitochondrial homeostasis following traumatic brain injury using the uncoupler FCCP. *Exp Neurol* 2009; **218**: 381–389.

33 Kawamata T, Katayama Y, Hovda DA, Yoshino A, Becker DP. Administration of excitatory amino acid antagonists via microdialysis attenuates the increase in glucose utilization seen following concussive brain injury. *J Cereb Blood Flow Metab* 1992; **12**: 12–24.

34 Semenza GL. Hypoxia-inducible factor 1: regulator of mitochondrial metabolism and mediator of ischemic preconditioning. *Biochim Biophys Acta* 2011; **1813**: 1263–1268.

35 Cartagena CM, Phillips KL, Tortella FC, Dave JR, Schmid KE. Temporal alterations in aquaporin and transcription factor HIF1alpha expression following penetrating ballistic-like brain injury (PBBI). *Mol Cell Neurosci* 2014; **60**: 81–87.

36 Zoltewicz JS, Mondello S, Yang B, Newsom KJ, Kobeissy F, Yao C et al. Biomarkers track damage after graded injury severity in a rat model of penetrating brain injury. *J Neurotrauma* 2013; **30**: 1161–1169.

37 Astrup J, Siesjo BK, Symon L. Thresholds in cerebral ischemia - the ischemic penumbra. *Stroke* 1981; **12**: 723–725.

38 Heiss WD. The ischemic penumbra: correlates in imaging and implications for treatment of ischemic stroke. The Johann Jacob Wepfer award 2011. *Cerebrovasc Dis* 2011; **32**: 307–320.

39 Wu HM, Huang SC, Vespa P, Hovda DA, Bergsneider M. Redefining the pericontusional penumbra following traumatic brain injury: evidence of deteriorating metabolic derangements based on positron emission tomography. *J Neurotrauma* 2013; **30**: 352–360.

40 Yao C, Wei G, Lu XC, Yang W, Tortella FC, Dave JR. Selective brain cooling in rats ameliorates intracerebral hemorrhage and edema caused by penetrating brain injury: possible involvement of heme oxygenase-1 expression. *J Neurotrauma* 2011; **28**: 1237–1245.